International Scholarly Research Network
ISRN Thermodynamics
Volume 2012, Article ID 917836, 11 pages
doi:10.5402/2012/917836

Research Article

Thermodynamics of f.c.c.-Ni–Fe Alloys in a Static Applied Magnetic Field

I. V. Vernyhora,[1,2] V. A. Tatarenko,[2] and S. M. Bokoch[3,4]

[1] *Department of Theoretical Physics, Institute for Applied Physics, N.A.S. of Ukraine, 58 Petropavlivska Street, 40030 Sumy, Ukraine*
[2] *Department of Solid State Theory, G. V. Kurdyumov Institute for Metal Physics, N.A.S. of Ukraine, 36 Academician Vernadsky Boulevard, 03680 Kyyiv-142, Ukraine*
[3] *Department of Materials Design and Technology, Institute for Advanced Materials Science and Innovative Technologies, 15 Sauletekio Avenue, 10224 Vilnius, Lithuania*
[4] *Department of Partial Differential Equations, Laboratoire Jean Kuntzmann, UMR 5224 CNRS, Tour IRMA, rue des Mathématiques 51, P.O. Box 53, 38041 Grenoble Cedex 9, France*

Correspondence should be addressed to S. M. Bokoch, sergiy.bokoch@gmail.com

Received 10 February 2012; Accepted 27 February 2012

Academic Editors: N. S. Ananikian, G. Maurin, B. Merinov, and S. Yulin

Within the scope of the self-consistent field and mean ("molecular") self-consistent field approximations, applying the static concentration wave method, the thermodynamics of f.c.c.-Ni–Fe alloys undergoing the static applied magnetic field effects is studied in detail. Under such conditions, the analytical corrections to expressions for the configuration-dependent part of free energy of macroscopically ferromagnetic $L1_2$-Ni_3Fe-type or $L1_0$-NiFe-type ordering phases are taken into account. The obtained results for thermodynamically equilibrium states are compared with the refined phase diagram for f.c.c.-Ni–Fe alloys calculated recently without taking into account the applied magnetic field effects. Considering the specific character of microscopic structure of the magnetic and atomic orders in f.c.c.-Ni–Fe alloys, the changes of shape (and in arrangement) of order-disorder phase-transformation curves (Kurnakov points) are thoroughly analysed. A special attention is addressed to the investigation of the concentration, temperature, and magnetic-field induction-dependent atomic and magnetic long-range order parameters, especially, near their critical points. As revealed unambiguously, influence of a static applied magnetic field promotes the elevation of Kurnakov points for all the atomically ordering phases that is in an overall agreement with reliable experimental data. On the base of revealed phenomenon, the magneto external field analog-to-digital converter of the monochromatic radiations (X-rays or thermal neutrons) is hypothesized as a claim.

1. Introduction

Due to unique physical properties, Ni–Fe alloys take one of the key places among the up-to-date materials of mechanical and instrument engineering, cutting-edge microelectronics components, and are commonly used as materials of constructional, precision, and magnetosensitive elements in numerous devices and mechanisms [1]. At present, it is ascertained that the majority of physical properties of these alloys are conditioned by the coexistence and significant interplay of spatial atomic-configuration and magnetic-moment orders [1].

Experimentally determined phase diagram of a Ni–Fe system (which is "metastable" due to the limited technical capabilities of experimental methods) was adapted in accordance with [2] (Figure 1) and shows that the temperature decrease results in two sequential phase transformations, namely, paramagnetic-ferromagnetic transition of the second kind (at the Curie points) and order-disorder transformation of the first kind (at the Kurnakov points) in accordance with the symmetries of $L1_2$-type or $L1_0$-type ordered and $A1$-type disordered phases. The ordered alloys with $L1_2$-type substitutional superstructure (which is unambiguously observed in experiments for Ni_3Fe stoichiometry and was theoretically predicted for $NiFe_3$ stoichiometry) and $L1_0$-type substitutional superstructure (with equiatomic NiFe composition) originate from the disordered ($A1$-type) f.c.c. solid solution (which is characterized by the atomic

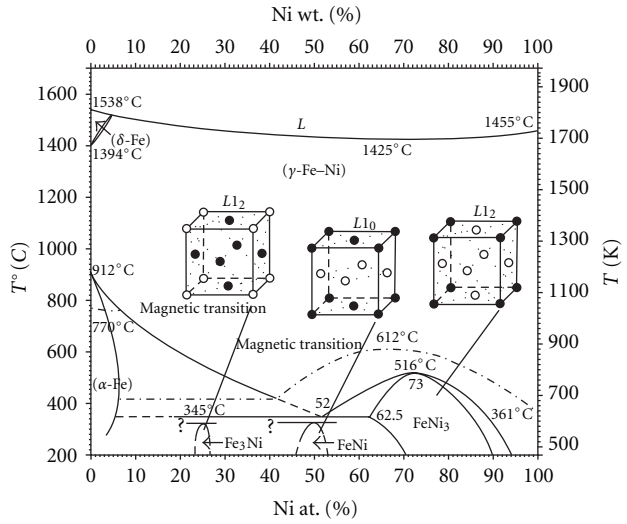

FIGURE 1: Experimentally obtained "metastable" phase diagram of Ni–Fe alloys (which is adapted in accordance with [2]). The symbol "?" denotes the unidentified authentically structural and/or magnetic states of alloys. γ-Fe, α-Fe, and δ-Fe are the f.c.c., low-, and high-temperature b.c.c. crystal lattice modifications of an iron. L is the Ni–Fe liquid solution. The equilibrium crystal structures of the three stoichiometric ordered phases at $T = 0$ K (from right to the left), $L1_2$-Ni_3Fe (Permalloy), $L1_0$-NiFe (Elinvar), and $L1_2$-$NiFe_3$ (Invar), are also shown ($\circ$ = Ni, $\bullet$ = Fe).

short-range order (SRO) only) depending on the Fe (Ni) concentration and external thermodynamic parameters such as temperature (T) and pressure (p) [1, 2].

As can be seen from phase diagram (Figure 1), both magnetic-transition and structural phase-transformation points, namely, the Curie and Kurnakov temperatures, decrease with increasing Fe concentration. Moreover, the reliable determination of the phase-equilibria boundaries below 600 K needs an additional long-duration experimental investigation and a respective theoretical evaluation. The former is difficult practically because, in the laboratory conditions, it is hindered to obtain atomically ordered samples of alloys at issue, especially with a nonstoichiometric composition, due to appreciable slowing down of the diffusion-controlled processes even at temperatures near 600–800 K.

As a rule, the magnetic nature of a Ni–Fe system is associated with Fe and Ni constituents belonging to the group of 3d-transition metals. Their magnetism appears due to the unfilled 3d-electron shell of atoms. The magnetic order naturally appears due to "exchange" interaction between the full ("effective") magnetic moments of such ions localized at the crystal-lattice sites and/or due to "exchange" interaction between the quasi-free conductivity electrons (known as "itinerant" magnetism). In addition, one should accept the possibility of the active influence of conductivity electrons on a system of uncompensated magnetic moments of the "formerly" localized 3d-electrons [1, 3, 4].

The numerous experimental data [1–3] confirm the wide concentration and temperature intervals of availability of the $L1_2$-Ni_3Fe-type ordered alloys well known as Permalloys. The most salient properties of these alloys are high magnetic permeability, low values of magnetic-anisotropy and magnetostriction parameters, and so forth [1, 3–7]. The availability of substitutional $L1_0$- and $L1_2$-type ordered (super)structures with NiFe and $NiFe_3$ stoichiometry, respectively, was reliably proven theoretically and confirmed experimentally by means of electron diffraction methods in the meteoritic samples with these compositions (the most known and studied alloy belongs to the Santa Catharina meteorite) [1, 8–12]. So-called Elinvar ($L1_0$-NiFe-type) alloys are noteworthy due to their unique elastic properties and, in particular, the precision stability of the elasticity (Young's) modulus within the certain temperature intervals [1, 13, 14] that caused their wide practical application in the spring materials for watches industry and related areas. In one's turn, Invar (Fe_3Ni-type) alloys (with $\cong$64–66 at.% of Fe according to the existent technological standards [1]) are characterized by low or even negative values of a thermal expansion coefficient [1, 8–12]. This well-known phenomenon is referred to as Invar effect.

Let us note that the Earth core and even a number of the Solar system celestial bodies consist of Ni–Fe alloys with the Ni concentration ranging from 5 to 15 at.% (see, e.g., a recent critical review [15]). Therefore, along with the exceptional practical importance of these materials, they are of a great interest for the Earth and Solar system physical investigations. As a result, the numerical and analytical studies of phase equilibria, order-disorder phase transformations, and decomposition reactions as well as kinetics of atomic ordering in Ni–Fe alloys under the extreme conditions (in particular, at high pressure and enhanced temperature) are important for interpretation or prediction of seismic and geomagnetic phenomena and may provide us a deeper understanding of the Earth interior properties.

In one's turn, the applied magnetic field can also significantly affect the equilibrium properties and critical-point effects of Ni–Fe alloys, in particular, the phase-transformation temperatures, the kinetics of time evolution of phase morphologies, and so forth. It was noted earlier [16] that the strong magnetic fields (up to 30–40 T) may significantly affect the phase transformations, similarly to high pressures or elevated temperatures. Previous investigations [17–19] proved that in f.c.c.-Ni–Fe and b.c.c.-Fe–Ni alloys with a high Fe content (>70 at.%) the starting temperature of martensitic transformation (f.c.c. $\leftrightarrow$ b.c.c. ($\gamma \leftrightarrow \alpha$)), T_M, increases under the influence of an applied magnetic field. Similar effect was observed in other practically important alloys, particularly, in Fe–Ni–C, Fe–Pt, and so forth [18–20]. Also, it was revealed that the magnetic field can change the morphology of the ferritic (α-Fe–C solid solution) grains in Fe–C alloys [20] as well as both the morphology and the roughness of the electrodeposited layers of a pure nickel and Ni–Fe alloys depending on the applied magnetic-field direction [21]. In Permalloy-type alloys, which have recently obtained their promising applications in both solid-state magnetic random access memory (MRAM) technology and magnetic logic [22, 23], the applied magnetic fields are commonly exploited to form or switch the predefined local magnetic structures, to control the movement of static (Bloch or Néel)

domain walls, and so forth. For such bulk crystal alloys, the recent Monte Carlo modelling predicts, for instance, the increase of the order-disorder phase-transformation temperature [24] when the applied magnetic field increases. It should be noted that the magnetic field effects are also revealed in nonmagnetic materials. For example, in zinc-based alloys and pure titanium, some texture appears under the magnetic field (see, e.g., [19]). Thus, the predictable and controllable influence of an applied magnetic field on the thermodynamic and kinetic properties of magnetic materials is of fundamental and practical interests.

In a given article, we consider the effects of a static applied magnetic field on the thermodynamics of f.c.c.-Ni–Fe alloys in concentration-temperature range of Elinvars (≅40–55 at.% of Fe) and Permalloys (≅20–35 at.% of Fe). In order to calculate a phase diagram, critical or phase-transformation temperatures and long-range order (LRO) parameters for both magnetic and atomic subsystems under these external conditions, the statistical-thermodynamics model is formulated in Section 2. The obtained results and discussion of them are given in Section 3, and the general conclusions are summarized in Section 4.

2. Statistical Thermodynamics Model of f.c.c.-Ni–Fe Alloys under the Influence of a Static Applied Magnetic Field

Following [15, 25–29], we consider a substitutional f.c.c.-Ni–Fe alloy, which consists of two magnetic constituents and is characterized by two types of a spatial order, notably, magnetic and atomic orders. It is worth noting that the presented analysis is based solely on the local magnetic moments model, which is valid within the lattice-gas approximation only and cannot be applied to the description of the "itinerant" magnetism of "quasi-free" electrons. Nonetheless, a reader can find both approaches and their comparative analysis based on a reciprocal-space symmetry consideration in recent critical reviews [27, 28]; the comprehensive list of references to the most salient literature on this matter can be found elsewhere [29].

Thus, the configuration-dependent part of the classical Heisenberg Hamiltonian of considered Ising-type interacting system can be presented in the form [16, 30] as follows:

$$\begin{aligned}\widehat{H}_{\text{conf}} &= \widehat{H}_{\text{chem}} + \widehat{H}_{\text{magn}} \\ &= \frac{1}{2}\sum_{\mathbf{r},\mathbf{r}'}\sum_{\alpha,\beta} W_{\alpha\beta}(\mathbf{r}-\mathbf{r}')c_\alpha(\mathbf{r})c_\beta(\mathbf{r}') \\ &\quad + \frac{1}{2}\sum_{\mathbf{r},\mathbf{r}'}\sum_{\alpha,\beta} J_{\alpha\beta}(\mathbf{r}-\mathbf{r}')\left(\widehat{\mathbf{S}}_\alpha(\mathbf{r})\cdot\widehat{\mathbf{S}}_\beta(\mathbf{r}')\right)c_\alpha(\mathbf{r})c_\beta(\mathbf{r}') \\ &\quad - \mu_B\sum_{\mathbf{r}}\sum_{\boldsymbol{\alpha}} g_\alpha\left(\mathbf{B}\cdot\widehat{\mathbf{S}}_\alpha(\mathbf{r})\right)c_\alpha(\mathbf{r}).\end{aligned} \tag{1}$$

In (1), $\widehat{H}_{\text{chem}}$ and $\widehat{H}_{\text{magn}}$ are the configuration Hamiltonians of the atomic and magnetic subsystems, respectively. The indices (α, β) designate the types of atoms (Fe, Ni), $c_\alpha(\mathbf{r})$ is a local random variable (1 or 0) of substitution of f.c.c.-lattice site $\mathbf{r}$ by an α atom, $\widehat{\mathbf{S}}_\alpha(\mathbf{r})$ is the spin operator of α atom situated at the site $\mathbf{r}$, μ_B is the Bohr magneton, g_α is the Landé factor of α atom. $J_{\alpha\beta}(\mathbf{r}-\mathbf{r}')$ and $W_{\alpha\beta}(\mathbf{r}-\mathbf{r}')$ are the magnetic ("exchange") and "paramagnetic" (actually "electrochemical" together with "strain-induced" [15, 25–29]) "pairwise" interatomic-interaction energies, respectively. One can see that, in (1), the possible influence of the applied magnetic field with induction $\mathbf{B}$ on the spatial configuration of ions by means of their magnetic moments is taken into account explicitly (see, for details, [3, 4, 15, 27, 28]).

From the chosen configuration Hamiltonian, one can proceed with the statistical thermodynamics description of the atomic and magnetic orders of an alloy by applying the self-consistent field (SCF) and mean self-consistent field (MSCF) approximations, respectively, [3, 4, 30–32] in a combination with the static concentration wave (SCW) method (see, e.g., [30, 32]). The formation of $L1_2$-Ni_3Fe-type or $L1_0$-NiFe-type ordered substitutional (super) structures from the f.c.c.-$A1$-type disordered solid solution in f.c.c.-$Ni_{1-c}Fe_c$ alloys is realized by means of the first-order phase transformation. As a result, using (1) and SCF-, MSCF-, SCW-based approaches and omitting the routine mathematical transforms, it is possible to write the expressions for the configuration-dependent part of the free energy for each ordered phase (at temperature $T \geq 0\,\text{K}$, composition c, and under a static applied magnetic field with induction B) in the following forms:

$$\begin{aligned}\frac{F_{\text{conf}}}{N_{\text{u.c.}}} &\cong \frac{\Delta U_{0\text{prm}}}{N_{\text{u.c.}}} \\ &\quad + \frac{c^2}{2}\Big[\widetilde{w}_{\text{prm}}(\mathbf{0}) + \widetilde{J}_{\alpha\alpha}(\mathbf{0})s_\alpha^2\sigma_\alpha^2 + \widetilde{J}_{\beta\beta}(\mathbf{0})s_\beta^2\sigma_\beta^2 \\ &\qquad \times\frac{(1-c)^2}{c^2} + 2\widetilde{J}_{\alpha\beta}(\mathbf{0})s_\alpha s_\beta\sigma_\alpha\sigma_\beta\frac{1-c}{c} \\ &\qquad + \frac{3}{16}\frac{\eta^2}{c^2}\left(\widetilde{w}_{\text{prm}}(\mathbf{k}_X) + \widetilde{J}_{\alpha\alpha}(\mathbf{k}_X)s_\alpha^2\sigma_\alpha^2\right. \\ &\qquad\qquad \left.+\widetilde{J}_{\beta\beta}(\mathbf{k}_X)s_\beta^2\sigma_\beta^2 - 2\widetilde{J}_{\alpha\beta}(\mathbf{k}_X)s_\alpha s_\beta\sigma_\alpha\sigma_\beta\right)\Big] \\ &\quad - \mu_B g B\left(cs_\alpha\sigma_\alpha + (1-c)s_\beta\sigma_\beta\right) + \frac{k_BT}{4} \\ &\quad \times\left[\left(c+\frac{3}{4}\eta\right)\ln\left(c+\frac{3}{4}\eta\right) + \left(1-c-\frac{3}{4}\eta\right)\right. \\ &\qquad \times\ln\left(1-c-\frac{3}{4}\eta\right) + 3\left(c-\frac{\eta}{4}\right)\ln\left(c-\frac{\eta}{4}\right) \\ &\qquad \left.+3\left(1-c+\frac{\eta}{4}\right)\ln\left(1-c+\frac{\eta}{4}\right)\right] \\ &\quad - k_BT\left\{c\left[\ln\,\text{sh}\frac{(2s_\alpha+1)\xi_\alpha\left(\sigma_{\alpha,\beta}\right)}{2s_\alpha} - \ln\,\text{sh}\frac{\xi_\alpha\left(\sigma_{\alpha,\beta}\right)}{2s_\alpha}\right.\right. \\ &\qquad \left.\left.-\xi_\alpha\left(\sigma_{\alpha,\beta}\right)\mathcal{B}_{s_\alpha}\left(\xi_\alpha\left(\sigma_{\alpha,\beta}\right)\right)\right] + (1-c)\right.\end{aligned}$$

$$\times\left[\ln\operatorname{sh}\frac{\left(2s_\beta+1\right)\xi_\beta\left(\sigma_{\beta,\alpha}\right)}{2s_\beta}-\ln\operatorname{sh}\frac{\xi_\beta\left(\sigma_{\beta,\alpha}\right)}{2s_\beta}-\xi_\beta\left(\sigma_{\beta,\alpha}\right)\mathcal{B}_{s_\beta}\left(\xi_\beta\left(\sigma_{\beta,\alpha}\right)\right)\right]\Bigg\}, \tag{2a}$$

or

$$\begin{aligned}\frac{F_{\text{conf}}}{N_{\text{u.c.}}}\cong{}&\frac{\Delta U_{0\text{prm}}}{N_{\text{u.c.}}}\\&+\frac{c^2}{2}\Bigg[\widetilde{w}_{\text{prm}}(\mathbf{0})+\widetilde{J}_{\alpha\alpha}(\mathbf{0})s_\alpha^2\sigma_\alpha^2\\&\quad+\widetilde{J}_{\beta\beta}(\mathbf{0})s_\beta^2\sigma_\beta^2\frac{(1-c)^2}{c^2}\\&\quad+2\widetilde{J}_{\alpha\beta}(\mathbf{0})s_\alpha s_\beta\sigma_\alpha\sigma_\beta\frac{1-c}{c}+\frac{1}{4}\frac{\eta^2}{c^2}\\&\quad\times\left(\widetilde{w}_{\text{prm}}(\mathbf{k}_X)+\widetilde{J}_{\alpha\alpha}(\mathbf{k}_X)s_\alpha^2\sigma_\alpha^2\right.\\&\qquad\left.+\widetilde{J}_{\beta\beta}(\mathbf{k}_X)s_\beta^2\sigma_\beta^2-2\widetilde{J}_{\alpha\beta}(\mathbf{k}_X)s_\alpha s_\beta\sigma_\alpha\sigma_\beta\right)\Bigg]\\&-\mu_B g B\left(cs_\alpha\sigma_\alpha+(1-c)s_\beta\sigma_\beta\right)+\frac{k_BT}{2}\\&\times\Bigg[\left(c+\frac{\eta}{2}\right)\ln\left(c+\frac{\eta}{2}\right)\\&\quad+\left(1-c-\frac{\eta}{2}\right)\ln\left(1-c-\frac{\eta}{2}\right)\\&\quad+\left(c-\frac{\eta}{2}\right)\ln\left(c-\frac{\eta}{2}\right)\\&\quad+\left(1-c+\frac{\eta}{2}\right)\ln\left(1-c+\frac{\eta}{2}\right)\Bigg]-k_BT\\&\times\Bigg\{c\left[\ln\operatorname{sh}\frac{(2s_\alpha+1)\xi_\alpha\left(\sigma_{\alpha,\beta}\right)}{2s_\alpha}-\ln\operatorname{sh}\frac{\xi_\alpha\left(\sigma_{\alpha,\beta}\right)}{2s_\alpha}\right.\\&\qquad\left.-\xi_\alpha\left(\sigma_{\alpha,\beta}\right)\mathcal{B}_{s_\alpha}\left(\xi_\alpha\left(\sigma_{\alpha,\beta}\right)\right)\right]+(1-c)\\&\quad\times\left[\ln\operatorname{sh}\frac{\left(2s_\beta+1\right)\xi_\beta\left(\sigma_{\beta,\alpha}\right)}{2s_\beta}-\ln\operatorname{sh}\frac{\xi_\beta\left(\sigma_{\beta,\alpha}\right)}{2s_\beta}\right.\\&\qquad\left.-\xi_\beta\left(\sigma_{\beta,\alpha}\right)\mathcal{B}_{s_\beta}\left(\xi_\beta\left(\sigma_{\beta,\alpha}\right)\right)\right]\Bigg\}.\end{aligned} \tag{2b}$$

Equation (2a) is suitable for $L1_2$-Ni_3Fe-type f.c.c.-Ni–Fe alloys (Permalloys; α = Fe, β = Ni) within the Ni-reach region; after some trivial replacement of indices ($\alpha \leftrightarrow \beta$), it can be adapted for $L1_2$-$NiFe_3$-type f.c.c.-Ni–Fe alloys (Invars) within the Fe-reach region. Equation (2b) is suitable for $L1_0$-NiFe-type f.c.c.-Ni–Fe alloys (Elinvars; α = Fe, β = Ni) near the equiatomic composition. Here, k_B is the Boltzmann constant; $g_{\text{Fe}} \cong g_{\text{Ni}} = g$. $\Delta U_{0\text{prm}}$ is the configuration-independent part of the internal energy, which is a linear function of a relative substitution-atom concentration, c (Fe in f.c.c.-Ni or Ni in f.c.c.-Fe). $N_{\text{u.c.}}$ is a total number of crystal-lattice sites (atoms) or primitive unit cells. Within the scope of the "pairwise" interatomic-interactions approximation, the Fourier component of "paramagnetic" "mixing" energies, $\widetilde{w}_{\text{prm}}(\mathbf{k})$, for any quasi-wave vector $\mathbf{k}$ in the first Brillouin zone (1st BZ) of a reciprocal space is defined as $\widetilde{w}_{\text{prm}}(\mathbf{k}) = \widetilde{W}_{\text{FeFe}}(\mathbf{k}) + \widetilde{W}_{\text{NiNi}}(\mathbf{k}) - 2\widetilde{W}_{\text{FeNi}}(\mathbf{k})$. $\widetilde{J}_{\alpha\beta}(\mathbf{k})$ is the Fourier transform of the real-space "exchange"-interaction energies, $J_{\alpha\beta}(\mathbf{r}-\mathbf{r}')$, which arise between the atoms with magnetic moments in α-β pairs. In many cases (for $L1_2$- or $L1_0$-type structures), the atomic LRO parameter, η, can be estimated experimentally. For this goal, we have to use the elastic X-rays or thermal-neutrons diffraction data, and the resulted LRO parameters are defined by the ratio of superstructure-to-structure reflection intensities. However, it should be mentioned that, due to closeness of the atomic scattering factors, $f_{\text{Fe}}(\mathbf{k})$ and $f_{\text{Ni}}(\mathbf{k})$, for X-rays (as well as for electronic waves, while neglecting the additional extraneous contribution of their significant dynamical-diffraction effects), such an experiment should be carried out at beam energies (wavelengths) close to the absorption edge of one of the constituents. This "trick" will increase the difference, $[(1-c)f_{\text{Ni}}(\mathbf{k}) - cf_{\text{Fe}}(\mathbf{k})]^2$, which determines the superstructural-reflection intensity. On the other hand, in case of elastic thermal-neutron scattering, this requirement is not necessary; nevertheless, in order to increase the diffracted-beam intensity, one should use the Ni–Fe alloy samples containing stable isotopes (in particular, ^{62}Ni atoms). σ_α is the magnetic LRO parameter (i.e., reduced magnetization per atom) of α-th atomic-moment subsystem; $\mathcal{B}_{J_\alpha}(\xi_\alpha)$ is the conventional Brillouin function [33, 34] defined as

$$\mathcal{B}_{J_\alpha}(\xi_\alpha)\equiv\left(1+\frac{1}{2J_\alpha}\right)\operatorname{cth}\left(\left(1+\frac{1}{2J_\alpha}\right)\xi_\alpha\right)-\frac{1}{2J_\alpha}\operatorname{cth}\left(\frac{1}{2J_\alpha}\xi_\alpha\right),$$

$$\xi_\alpha\equiv\frac{J_\alpha\left(H_{\text{mol}}^\alpha+H_{\text{ext}}\right)}{k_BT}\cong\frac{J_\alpha g\mu_B}{k_BT}\left(-\sum_\beta\Gamma_{\alpha\beta}\sigma_\beta+B\right). \tag{3}$$

Here, $J_\alpha = s_\alpha + l_\alpha$ is the total angular momentum of α atom; it consists of both the spin number (s_α) and the orbital momentum number (l_α). We assume that, for transition metals, $J_\alpha \cong s_\alpha (g \cong 2)$. $\mathbf{H}_{\text{ext}}$ is the applied magnetic field with induction $\mathbf{B}$; $H_{\text{mol}}^\alpha \cong -g\mu_\beta \sum_\beta \Gamma_{\alpha\beta}\sigma_\beta$ is the Weiss intracrystalline "molecular" field (MSCF) with coefficients $\{\Gamma_{\alpha\beta}\}$.

The equilibrium values of LRO parameters, η, σ_α, and σ_β (α = Fe, β = Ni), can be defined as solution of following set of transcendental equations:

$$\ln\frac{(c-(\eta/4))(1-c-(3/4)\eta)}{(1-c+(\eta/4))(c+(3/4)\eta)} = \frac{\eta}{k_BT}\Big[\widetilde{w}_{\mathrm{prm}}(\mathbf{k}_X)+\widetilde{J}_{\alpha\alpha}(\mathbf{k}_X)s_\alpha^2\sigma_\alpha^2+\widetilde{J}_{\beta\beta}(\mathbf{k}_X)s_\beta^2\sigma_\beta^2 -2\widetilde{J}_{\alpha\beta}(\mathbf{k}_X)s_\alpha s_\beta\sigma_\alpha\sigma_\beta\Big],$$

$$\sigma_\alpha = \mathcal{B}_{s_\alpha}\Big(-\frac{1}{ck_BT}\Big\{\widetilde{J}_{\alpha\alpha}(\mathbf{0})c^2s_\alpha^2\sigma_\alpha+\widetilde{J}_{\alpha\beta}(\mathbf{0}) \times c(1-c)s_\alpha s_\beta\sigma_\beta + \frac{3\eta^2\Big[\widetilde{J}_{\alpha\alpha}(\mathbf{k}_X)s_\alpha^2\sigma_\alpha-\widetilde{J}_{\alpha\beta}(\mathbf{k}_X)s_\alpha s_\beta\sigma_\beta\Big]}{16} -\mu_Bgcs_\alpha B\Big\}\Big),$$

$$\sigma_\beta = \mathcal{B}_{s_\beta}\Big(-\frac{1}{(1-c)k_BT}\Big\{\widetilde{J}_{\beta\beta}(\mathbf{0})(1-c)^2s_\beta^2\sigma_\beta+\widetilde{J}_{\alpha\beta}(\mathbf{0}) \times c(1-c)s_\beta s_\alpha\sigma_\alpha + \frac{3\eta^2\Big[\widetilde{J}_{\beta\beta}(\mathbf{k}_X)s_\beta^2\sigma_\beta-\widetilde{J}_{\alpha\beta}(\mathbf{k}_X)s_\beta s_\alpha\sigma_\alpha\Big]}{16} -\mu_Bg(1-c)s_\beta B\Big\}\Big), \tag{4a}$$

or

$$\ln\frac{(c-(\eta/2))(1-c-(\eta/2))}{(1-c+(\eta/2))(c+(\eta/2))} = \frac{\eta}{k_BT}\Big[\widetilde{w}_{\mathrm{prm}}(\mathbf{k}_X)+\widetilde{J}_{\alpha\alpha}(\mathbf{k}_X)s_\alpha^2\sigma_\alpha^2+\widetilde{J}_{\beta\beta}(\mathbf{k}_X)s_\beta^2\sigma_\beta^2 -2\widetilde{J}_{\alpha\beta}(\mathbf{k}_X)s_\alpha s_\beta\sigma_\alpha\sigma_\beta\Big],$$

$$\sigma_\alpha = \mathcal{B}_{s_\alpha}\Big(-\frac{1}{ck_BT}\Big\{\widetilde{J}_{\alpha\alpha}(\mathbf{0})c^2s_\alpha^2\sigma_\alpha+\widetilde{J}_{\alpha\beta}(\mathbf{0}) \times c(1-c)s_\alpha s_\beta\sigma_\beta + \frac{\eta^2}{4}\Big[\widetilde{J}_{\alpha\alpha}(\mathbf{k}_X)s_\alpha^2\sigma_\alpha-\widetilde{J}_{\alpha\beta}(\mathbf{k}_X)s_\alpha s_\beta\sigma_\beta\Big] -\mu_Bgcs_\alpha B\Big\}\Big),$$

$$\sigma_\beta = \mathcal{B}_{s_\beta}\Big(-\frac{1}{(1-c)k_BT}\Big\{\widetilde{J}_{\beta\beta}(\mathbf{0})(1-c)^2s_\beta^2\sigma_\beta+\widetilde{J}_{\alpha\beta}(\mathbf{0}) \times c(1-c)s_\beta s_\alpha\sigma_\alpha + \frac{\eta^2\Big[\widetilde{J}_{\beta\beta}(\mathbf{k}_X)s_\beta^2\sigma_\beta-\widetilde{J}_{\alpha\beta}(\mathbf{k}_X)s_\beta s_\alpha\sigma_\alpha\Big]}{4} -\mu_Bg(1-c)s_\beta B\Big\}\Big), \tag{4b}$$

for $L1_2$-Ni_3Fe-type (or $L1_2$-Fe_3Ni-type) and $L1_0$-NiFe-type ordered phases, respectively. Equations (4a) and (4b) are obtained by the differentiation of expression (2a) and (2b) with respect to order parameters, η, σ_{Fe}, and σ_{Ni}. Such equations neglecting the influence of an applied magnetic field can be found elsewhere [15, 25–29].

Thus, using (2a), (2b), (4a), and (4b) and knowing the quantitative information about the Fourier components of "paramagnetic" interatomic "mixing" and magnetic-moment "exchange" energies (for two quasi-wave vectors, $\mathbf{k}_\Gamma(000)$ and $\mathbf{k}_X(001)$, in the 1st BZ only), in particular, about their temperature-concentration dependences, one can estimate the critical-point and equilibrium parameters for f.c.c.-Ni–Fe alloys within the whole (T-c)-domain under the influence of a static applied magnetic field.

Let us point out that the solutions of transcendental Equations (4a) and (4b) can have irregularity points (due to breaks, discontinuities, or jumps) in their T and c dependences. There are, at least, two reasons of these irregularities. The first reason is attributed to a nonlinear character of transcendental-equations solution, which aggravates a singularity at approaching to the stoichiometric compositions such as $c = 1/2$ or $1/4(3/4)$ and temperatures close to 0 K. The second reason appears within the metastability region and at the critical points of the first-order phase transformation and the second-order phase transition (the Kurnakov and Curie temperatures), respectively. Therefore, during numerical calculations, all the solutions of transcendental Equations (4a) and (4b) should be determined with a caution near the singular and critical points.

In order to overcome the first reason of computational complexities, one can use the results proposed in [34–38]. Considering the interacting magnetic-moments subsystem only, the authors [35–38] proposed to pass from the transcendental Brillouin function to its parameterized polynomial approximation (as it was commonly done in a classical paramagnetism description by expanding the Langevin function; for details, see an exhaustive analysis in [34]). Using such a reasonable simplification, the authors have investigated the magnetic subsystem in crystalline and amorphous solids [38], taking into account their magnetic anisotropy and magnetostriction. The striking agreement with reliable experimental data for such systems was obtained. In addition, they have studied the critical behaviour of ferromagnetic materials [39] and, notably, the critical exponents of a static magnetic susceptibility. Subsequently, the elegant theory of

transitions accompanied with spin reorientation has been developed on the basis of proposed earlier approaches. The influence of applied magnetic field on these transitions has also been investigated [40].

Without underestimating the essential role of ideas proposed in [34–38], one should note that such an approach has some disadvantages in view of the second reason of above-mentioned problem. In particular, an expansion of the Brillouin function, $\mathcal{B}_{J_\alpha}(\xi_\alpha)$, into the Maclaurin series is reasonable for small values of the argument ξ only [33, 34], that is, at high temperatures or weak "exchange" interaction between the magnetic moments. This does not always satisfy the actual alloy requirements and the practical interests. In particular, in case of the substantial mutual influence of magnetic and atomic subsystems of alloys at issue, such an approach becomes even useless. By means of the imitation of f.c.c.-Ni–Fe alloys, one can demonstrate, taking into account the certain physical conditions, that there is a successful application of (4a) and (4b) for the whole (T-c)-domain, for instance, without using the asymptotic relation presented in [34–38]. In f.c.c.-Ni–Fe alloys, the paramagnetic-ferromagnetic phase transitions at the Curie points, $T_C(c)$, are of the second kind, and the $A1 \leftrightarrow L1_2$ ($L1_0$) structural transformations at the Kurnakov temperatures, $T_K(c)$, are of the first kind (though, in some certain cases, it can be close to the second kind); therefore, due to the jump of the atomic LRO parameter, $\Delta\eta(T_K)$, at the Kurnakov point precisely, the magnetizations of nickel (σ_{Ni}) and iron (σ_{Fe}) subsystems also undergo the jumps, $\Delta\sigma_{\mathrm{Ni,Fe}}(T_K)$ [26].

3. Results and Discussion

For numerical calculations of (2a), (2b), (4a), and (4b), it is necessary to know the Fourier components of energy parameters of interatomic interactions, namely, "paramagnetic" ("electrochemical" together with "strain-induced") and magnetic ones [15, 25–28]. The former (considering the contribution of the latter to the alloy thermodynamics and vice versa) can be evaluated by means of the well-known Krivoglaz-Clapp-Moss formula (see [15, 25–28] and references therein), using the experimental data on elastic diffuse scattering of radiations from disordered alloys (with atomic SRO only). This classical formula explicitly ties up the microscopic energy parameters of the alloy (its "mixing" energies) and SRO parameters or, more specifically, the X-rays or thermal neutrons diffuse scattering intensities. Recently, in [26, 27], within the scope of the analysis of reliable diffraction data for f.c.c.-$\mathrm{Ni}_{1-c}\mathrm{Fe}_c$ alloys, the authors suggested the polynomial approximation for estimation of the "paramagnetic" "mixing"-energy Fourier components for a few related quasi-wave vectors in the 1st BZ as follows:

$$\widetilde{w}_{\mathrm{prm}}(\mathbf{k}, c) \cong K_0(\mathbf{k}) + K_1(\mathbf{k})c + K_2(\mathbf{k})c^2. \quad (5)$$

The values of $K_m(\mathbf{k})$ ($m = 0, 1, 2$) are listed in Table 1 according to [27].

The Fourier components of "exchange" interaction parameters can be estimated, using the experimental data about the Curie temperatures for various Fe-concentrations in an alloy, $T_C = T_C(c)$. Self-consistently calculated values of these parameters for high-symmetry points $\Gamma(000)$ and $X(001)$ in a reciprocal space are given in Table 2 (for details, see [26–28]).

Table 1: The coefficients, $K_0(\mathbf{k})$, $K_1(\mathbf{k})$, and $K_2(\mathbf{k})$ in [eV], which enter into (5) for the estimation of concentration-dependent "paramagnetic" "mixing"-energies Fourier components for two quasi-wave vectors $\mathbf{k}_\Gamma(000)$ and $\mathbf{k}_X(100)$ for f.c.c.-$\mathrm{Ni}_{1-c}\mathrm{Fe}_c$ alloys (according to [27]).

$\mathbf{k}$	$K_0(\mathbf{k})$	$K_1(\mathbf{k})$	$K_2(\mathbf{k})$
$\Gamma(000)$	0.843	−2.339	2.344
$X(100)$	−0.414	0.450	—

Using the above-mentioned parameters of interatomic interactions (see Tables 1 and 2), the sets of (4a) and (4b) can be solved numerically using the modified Newton method. As a result, neglecting or taking into account a static applied magnetic field with induction $\mathbf{B}$, one can obtain the equilibrium and static critical-point parameters for f.c.c.-$\mathrm{Ni}_{1-c}\mathrm{Fe}_c$ alloys within the concentration interval of $c \in [0.005; 0.6]$. For performed calculations, it was assumed that the magnitude of applied field, B, changes from 0 T to 50 T. The choice of 50 T as a maximum value of B was stipulated by a maximum field magnitude, which can be reached nowadays in the laboratory conditions [41].

From Table 2, one can see that the "exchange" interaction Fourier components, $\widetilde{J}_{\mathrm{NiNi}}(\mathbf{k})$ and $\widetilde{J}_{\mathrm{FeNi}}(\mathbf{k})$, correspond to the ferromagnetic interaction between the magnetic moments in Ni–Ni and Fe–Ni atomic pairs, and $\widetilde{J}_{\mathrm{FeFe}}(\mathbf{k})$ corresponds to the antiferromagnetic interaction between the magnetic moments in Fe–Fe atomic pairs. This result is in an excellent agreement with many experimental findings for f.c.c.-Ni–Fe alloy (for details, see analysis in [26–28]). The solutions of (4a) and (4b) are the LRO parameters, $\eta(c, B, T)$, $\sigma_{\mathrm{Ni}}(c, B, T)$, $\sigma_{\mathrm{Fe}}(c, B, T)$, and consequently they were used for calculation of the respective curves of configuration-dependent part of free energy (2a) and (2b) $F_{\mathrm{conf}}(c, B, T)$ for $A1$-, $L1_2$-, and $L1_0$-type ferromagnetic phases. The phase diagram for certain concentration interval, temperature and applied magnetic field magnitude can be plotted after the evaluation of existence regions for homogeneous phases and coexistence regions of two phases in a mixture under equilibrium conditions. These intervals have been defined from the free energy curves by applying the common tangent method.

In Figure 2, the results of such a phase-diagram construction for f.c.c.-Ni–Fe alloys are shown for two cases with neglecting ($B = 0$ T, Figure 2(a)) and taking into account a static applied magnetic field ($B = 50$ T, Figure 2(b)). Because of the applied magnetic-field influence, one can notice the changes of phase boundaries geometry, namely, both the decrease of an area of some phase-mixture regions (in particular, Fe-rich $L1_2 + A1$ mixture at enhanced temperatures) and the increase of order-disorder phase-transformation temperatures for all ordering structures. Undoubtedly, these macroscopic effects are conditioned by a microscopic nature of the system at issue. For instance, as shown recently in [26–28], both the "paramagnetic" "mixing" energies Fourier

Table 2: The "exchange" (magnetic) interaction energies Fourier components in [meV] for two quasi-wave vectors $\mathbf{k}_\Gamma(000)$ and $\mathbf{k}_X(100)$ for f.c.c.-Ni–Fe alloys (according to [26, 27]).

s_{Ni}	s_{Fe}	$\widetilde{J}_{NiNi}(\mathbf{0})$	$\widetilde{J}_{FeFe}(\mathbf{0})$	$\widetilde{J}_{FeNi}(\mathbf{0})$	$\widetilde{J}_{NiNi}(\mathbf{k}_X)$	$\widetilde{J}_{FeFe}(\mathbf{k}_X)$	$\widetilde{J}_{FeNi}(\mathbf{k}_X)$
1/2	3/2	−215.9	54.9	−231.5	72.0	−18.3	77.2

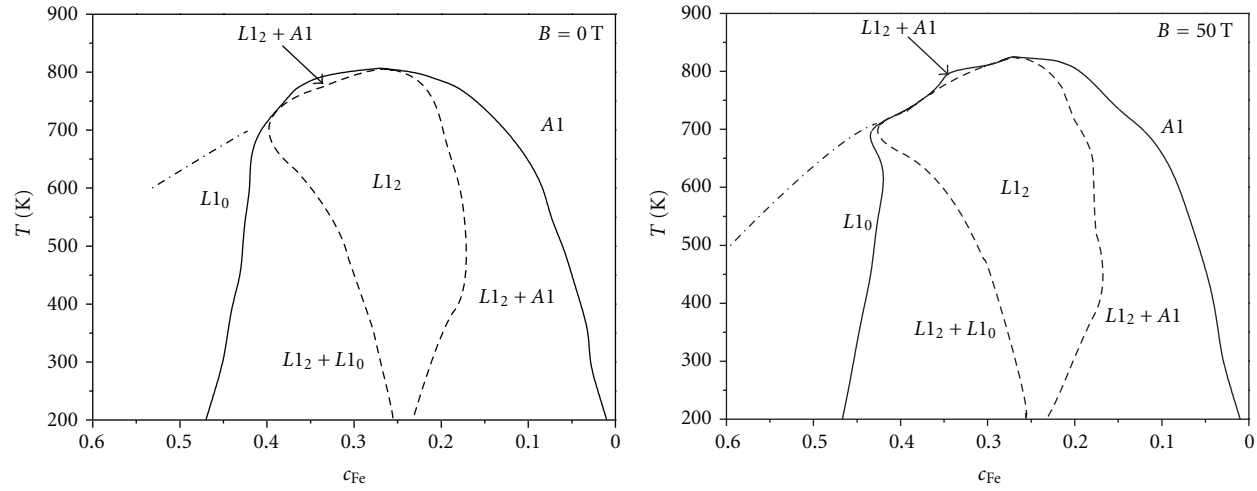

Figure 2: Calculated phase diagram of f.c.c.-Ni–Fe alloys ($c_{Fe} = c$) without (a) (see also [26]) and with (b) influence of a static applied magnetic field of induction $B = 0$ T and $B = 50$ T, respectively.

component and the "exchange" "mixing" energies Fourier component have the same negative sign for the superstructural wave-vector $\mathbf{k}_X(001)$ of a reciprocal space, and, as a result, in a ferromagnetic state of alloys, the depth of the total "mixing" energy will increase with a temperature decreasing. When the external magnetic field is applied, such an effect will be more pronounced.

The Kurnakov temperature dependences on both the alloy concentration and the applied magnetic-field magnitude are shown in Figure 3. The increase of $T_K(c, B)$ for both ordering structures of $L1_2$ (Figure 3(a)) or $L1_0$ (Figure 3(b)) types is observed with increase of the static applied magnetic-field induction, B. Thus, the previous conclusion is valid again.

In Figure 4, one can find the comparison of the $T_K = T_K$ ($c = \text{const}$, B) plots at $c = 0.25$ obtained in a given work and earlier by means of the Monte Carlo (MC) simulation [24]. It should be noted that, regardless the type of a model, the generally increasing behaviour of Kurnakov points with an increase of a static applied magnetic field is observed. The quantitative disagreement of the outputs estimated by the MC simulation [24] and the presented SCF + MSCF calculation can be explained by two primary reasons. (I) There is a difference in the interatomic-interaction parameters (of both "paramagnetic" and magnetic contributions) conditioned by the differences in used techniques of their estimations, particularly, by a difference of the atomic spin-number magnitudes. (II) There are some principal differences in these methodologies, so far as self-consistent field approaches neglect the correlation of the spatial-distribution fluctuations (competing with $\mathbf{H}_{ext}$) but take into account the infinite range of interactions by means of the calculation of respective parameters within the reciprocal-space representation, whereas the MC method takes into account such correlation effects naturally but here the effective radius of interactions is limited to several coordination shells only (e.g., to the first shell, as in [24]). Besides, in the MC simulation, the finite-size effects in a modelling crystallite can influence the obtained result that is not the case for the self-consistent field smoothing in a far (statistical-thermodynamic) asymptotics. As we do not aim to compare extensively both these methods, we should focus only on the obtained qualitative agreement; the results of both examinations confirm again that, for macroscopically ferromagnetic f.c.c.-Ni–Fe alloys, a static magnetic field promotes the elevation of $L1_2$-order-disorder transformation points.

In consequence of the magnetic field influence, the character of concentration and temperature dependences of LRO parameters of a system, namely, atomic (η) and magnetic (σ_{Fe} and σ_{Ni}) ones, are changed too. Such changes are illustrated in Figure 5 where the LRO-parameters plots for $L1_2$-Ni–Fe-type structure are presented at $T = 780$ K and 810 K, which are below and above the Kurnakov point for the stoichiometric Ni_3Fe Permalloy ($T_K \approx 806$ K) calculated without taking into account the applied magnetic field ($B = 0$ T).

From the concentration and field dependences of $L1_2$-type atomic LRO parameter, η (Figures 5(a) and 5(d)), one can notice the broadening of the respective phase-existence concentration intervals with the increasing of the Kurnakov temperatures. This appears owing to increase of the magnetic-filed magnitude. For instance, at the absence of magnetic field, the stoichiometric Ni_3Fe alloy is completely

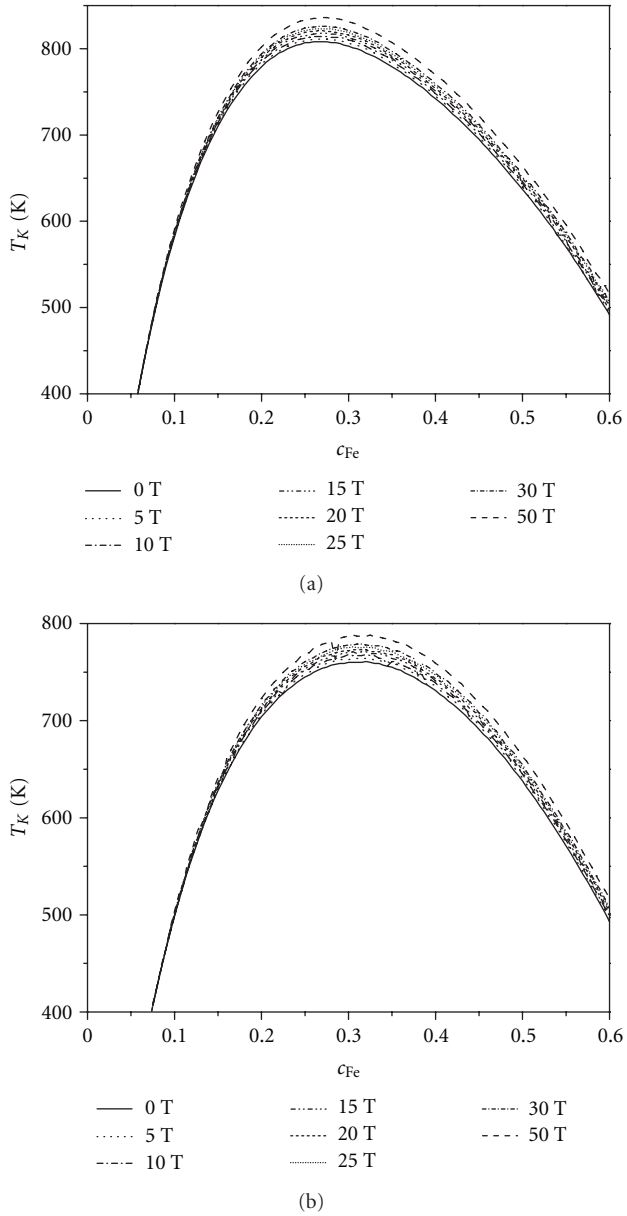

Figure 3: The Kurnakov temperature (T_K) dependences on concentration of Fe ($c_{Fe} = c$) at a static applied magnetic field of induction B for $L1_2$-Ni_3Fe-type (a) and $L1_0$-NiFe-type (b) ordering macroscopically ferromagnetic phases.

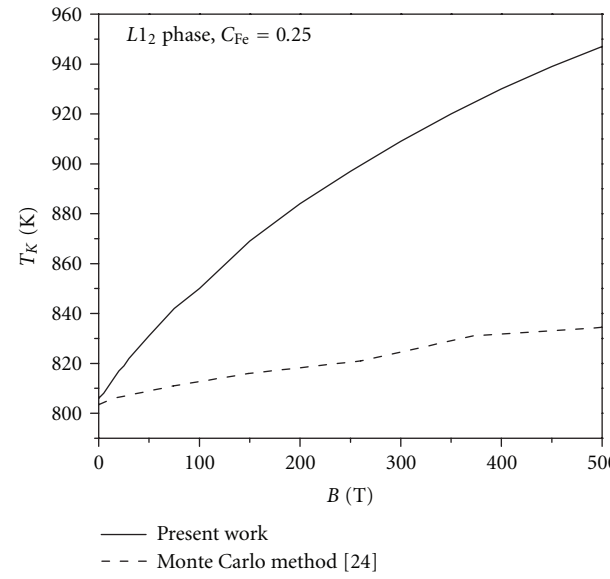

Figure 4: Comparison of the Kurnakov temperature dependences, T_K ($c = 0.25$, B), obtained by the Monte Carlo method [24] and, in a given work, by means of the SCF and MSCF approximations. The maximum tolerable magnetic induction is considered as $B_{max} = 500$ T to demonstrate only tendency of the T_K ($c = 0.25$, B) function (it does not relate to a real technical capability; see [41] for details).

disordered (f.c.c.-$A1$-type solid solution with atomic SRO only) at $T = 810$ K, and it becomes partly ordered ($\eta < 1$) in accordance with $L1_2$ type in consequence of application of a static magnetic field with the magnitude over 10 T.

Due to substantial interplay of magnetic and atomic subsystems, such changes of the atomic LRO parameters, $\eta(c, B)$ (Figures 5(a) and 5(d)) result in changes of magnetization curves of each magnetic subsystem separately, $\sigma_{Ni}(c, B)$ and $\sigma_{Fe}(c, B)$ (Figures 5(b) and 5(c) or 5(e) and 5(f)). The differences between the values of the relative magnetization change, $\{\sigma_{Ni,Fe}(c, B) - \sigma_{Ni,Fe}(c, 0)\}/\sigma_{Ni,Fe}(c, 0)$, and the $\sigma_{Ni,Fe}$ ($c = \text{const}, B$) curves for two studied temperatures, below (780 K) and above (810 K) the Kurnakov temperature, T_K ($c = 0.25$, 0 T) ≈ 806 K, are generally caused by the presence or absence of atomic LRO at these temperatures, respectively. Therefore, it unambiguously confirms again the perceptible influence of the atomic subsystem on the magnetic one and vice versa.

On the other hand, one can see that the $\sigma_{Ni,Fe}$ (c, B = const) dependences (Figures 5(b), 5(c), 5(e), and 5(f)) can have a "two-dome" shape. Central (upper) "dome" is situated in the vicinity of the stoichiometric Ni_3Fe composition ($c = 0.25$) and corresponds to the magnetization of the atomically ordered state of an alloy (when $\eta > \Delta\eta|T_K \neq 0; \Delta\eta|_{T_K}$ is a jump of the atomic LRO parameter at T_K). Lower "dome" (wider as regards concentration) corresponds to the magnetization in the absence of the atomic LRO ($\eta \equiv 0$).

Therefore, for each isomagnetic dependences, $\sigma_{Ni,Fe}$ (c, B = const), there are two breakpoints (to the left and to the right with respect to $c = 0.25$), at which the magnetizations undergo the finite jumps. These jumps are naturally conditioned by the atomic LRO-parameter jumps (at the Kurnakov points) caused by the influence of the applied magnetic field of a certain magnitude (above some critical value: $|\mathbf{B}| > B_c$). (An exhaustive analysis of the values and character of jumps, $\Delta\eta(c)|_{T_K}$ and $\Delta\sigma_{Ni,Fe}(c)|_{T_K}$, for both subsystems in the absence of an applied magnetic field can be found elsewhere [26]).

In conclusion, let us note that the authors of [16–20] have already mentioned that the applied magnetic field should be added to the list of the known thermodynamic variables.

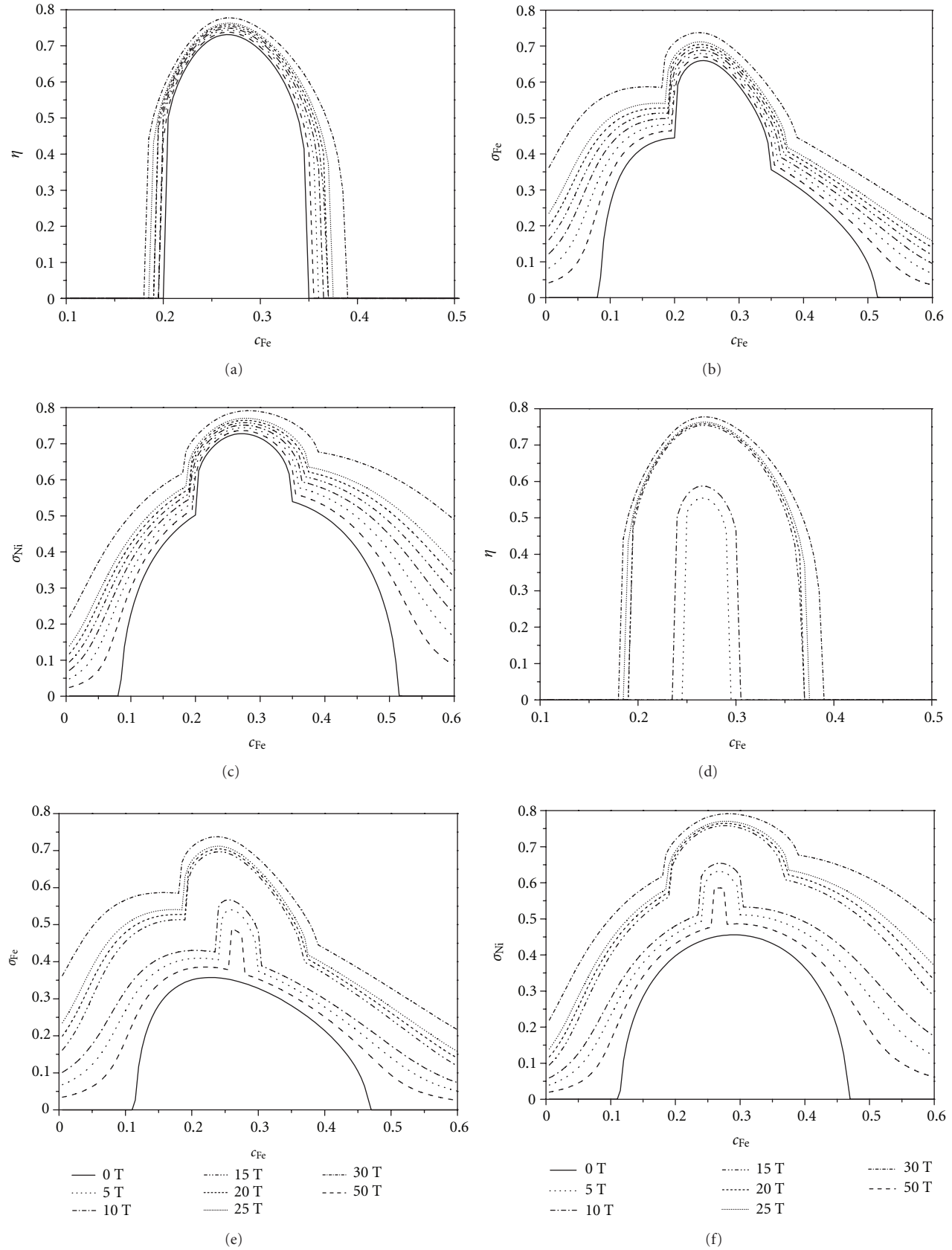

Figure 5: The calculated concentration ($c_{Fe} = c$) and magnetic-field (B) dependences of LRO parameters for atomic (η; (a), (d)) and magnetic, separately for nickel (σ_{Ni}; (c), (f)) and iron (σ_{Fe}; (b), (e)), subsystems in $L1_2$-Ni_3Fe-type phase at $T = 780$ K (a)–(c) or 810 K (d)–(f).

They also showed examples where the application of an external magnetic field results in the new T-c paths of an alloy evolution.

Commonly, Ni–Fe alloys are subjected to magnetic field during their exploitation (by the magnetic field of the Earth) and in the laboratory experiments too (up to 50 T). Small magnetic fields are used at annealing of soft magnetic materials for generating the predefined modification of the local atomic environment and nanoscale domain structures [1, 3, 5, 6, 22, 23].

The evaluation of thermodynamic changes induced by the applied magnetic-field effects on the local magnetic moments showed [17] that the magnetic field with the magnitude of 1 T changes the free energy of b.c.c.-Fe-based alloy approximately by the same amount as the temperature changed by 1 K. Therefore, as expected, using the experimentally attained fields of 30–40 T [41] one can reach the same effect as with the temperature changed by 30–40 K. From this point of view, there are several possible ways, by which the applied magnetic field can influence on the quantitative pattern of an alloy microstructure.

4. Summary

In a given article, the statistical-thermodynamics analysis of f.c.c.-Ni–Fe alloy under the influence of a static applied magnetic field has been carried out within the scope of the SCF and MSCF approximations [15, 25–28] taking into account both the spatial atomic order and the magnetic order, respectively. The comparison of two-phase equilibrium diagrams (with and without the applied magnetic field [26]; see also Figure 4) demonstrates that the applied magnetic field promotes the elevation of order-disorder phase-transformation points and the respective phase boundaries of atomically disordered phase (ferromagnetic f.c.c.-$A1$-type solid solution) and $L1_2$-Ni_3Fe- and $L1_0$-NiFe-type ordering structures. Such tendencies at the equilibrium conditions are in an overall agreement with the known experimental data and with the computational results for f.c.c.-Ni–Fe alloys [17–19, 42, 43] as well as the Heusler Ni–(Fe,Mn)–Ga alloys [44]. Thus, the main results of a given work demonstrate the principal possibility to elevate the Kurnakov phase-transformation points of ferromagnetic alloys under a static applied magnetic field. This can be successfully used for industrial ferromagnetic materials in order to enhance their thermal stability and, hence, to improve their operating characteristics under the extreme exploitation conditions.

Finally, one can foresee that the effect of jump-like changes of the atomic LRO, $\Delta\eta(c = \text{const}, B)|_{T_K}$ (Figure 5(d)), under the fields higher than some critical value ($B_c \cong 10$ T for compositions near the Ni_3Fe at $T \approx 810$ K) can be potentially used for design of the magnetosensitive sensor in order to transform the continuous and monochromatic radiations (such as synchrotron-based X-rays or nuclear-based neutrons) into the pulse mode. For instance, an application of the pulsed magnetic field with the amplitude $|\mathbf{B}| > B_c$ to a single-crystalline f.c.c.-$Ni_{1-c}Fe_c$ alloy (which is used as a crystal-monochromator or crystal-analyser aligned in accordance with the Bragg diffraction scheme with respect to the $(001)^*$-type superstructural reflection at $T > T_K$) allows to get the output signal (of diffracted intensity) in a pulse form. The technical parameters of this switching will be completely determined by the dynamics of jump-like changes of the $L1_2$-type atomic LRO, $\Delta\eta\ (c = \text{const}, B)|_{T_K}$, at the Kurnakov points, T_K ($c = \text{const}$, B). Moreover, the value of $\Delta\eta\ (c = \text{const}, B_c)|_{T_K}$ can reach $\cong 0.47$ (for the stoichiometric Ni_3Fe Permalloy; see references in [15, 25, 26, 31]), and, in this case, the signal-to-noise ratio may be sufficient for interrupted operation of the suggested analog-to-digital converter. In addition, such a single-crystalline sensor may be also used for precise detection of (ultra)high magnetic fields.

Acknowledgments

S. Bokoch would like to thank the Foundation Nanosciences (France) as well as the Institute for Advanced Materials Science and Innovative Technologies (Lithuania) for partial financial support of a given work.

References

[1] G. Béranger, F. Duffault, J. Morlet, J.-F. Tiers, and J. Friedel, *Les alliages de fer et de nickel: cent ans après la découverte de l'Invar*, Technique & Documentation, New York, NY, USA, 1996.

[2] T. B. Massalski, J. L. Murray, L. H. Bennett, and H. Baker, *Binary Alloy Phase Diagrams*, vol. 1, American Society for Metals, Metals Park, CA, USA, 1st edition, 1986.

[3] S. V. Vonsovskii, *Magnetism*, Nauka, Moscow, Russia, 1971.

[4] D. C. Mattis, *The Theory of Magnetism*, vol. 17 of *Springer Series in Solid-State Sciences*, Springer, New York, NY, USA, 1981.

[5] R. M. Bozorth, "Magnetism," *Reviews of Modern Physics*, vol. 19, no. 1, pp. 29–86, 1947.

[6] R. M. Bozorth, "The permalloy problem," *Reviews of Modern Physics*, vol. 25, no. 1, pp. 42–48, 1953.

[7] A. T. English and G. Y. Chin, "Metallurgy and magnetic properties control in permalloy," *Journal of Applied Physics*, vol. 38, no. 3, pp. 1183–1187, 1967.

[8] C.-W. Yang and J. I. Goldstein, "Phase decomposition of invar alloys. Information from the study of meteorites," in *The Invar Effect: A Centennial Symposium*, J. Wittenauer, Ed., pp. 137–146, The Minerals, Metals & Materials Society, Philadelphia, PA, USA, 1997.

[9] P. R. Munroe and M. Hatherly, "Observation of a $L1_2$ superlattice in Fe_3Ni," *Scripta Metallurgica et Materiala*, vol. 32, no. 1, pp. 93–97, 1995.

[10] E. F. Wassermann, "The invar problem," *Journal of Magnetism and Magnetic Materials*, vol. 100, no. 1–3, pp. 346–362, 1991.

[11] E. F. Wassermann, "Invar and anti-invar effect: finally understood after 100 years?" in *The Invar Effect: A Centennial Symposium*, J. Wittenauer, Ed., pp. 51–62, The Minerals, Metals & Materials Society, Philadelphia, PA, USA, 1997.

[12] A. P. Miodownik, "The concept of two gamma states," in *Physics and Application of Invar Alloys*, H. Saito et al., Ed., no. 3 of *Honda Memorial Series on Material Science*, chapter 12, pp. 288–310, Maruzen Company, Ltd., Tokyo, Japan, 1978.

[13] E. F. Wasserman, "Invar: moment-volume instabilities in transition metals and alloys," in *Ferromagnetic Materials*, K. H. J. Buschow and E. P. Wohlfarth, Eds., vol. 5, pp. 237–322, Elsevier, Elsevier, Amsterdam, The Netherlands, 1st edition, 1990.

[14] E. Z. Valiev, "Phenomenological theory of magnetoelastic interactions in invars and elinvars," *Soviet Physics Uspekhi*, vol. 34, no. 8, pp. 685–704, 1991.
[15] T. M. Radchenko and V. A. Tatarenko, "Fe–Ni alloys at high pressures and temperatures: statistical thermodynamics and kinetics of the $L1_2$ or $D0_{19}$ atomic order," *Uspehi Fiziki Metallov*, vol. 9, no. 1, pp. 1–170, 2008.
[16] M. A. Krivoglaz and V. D. Sadovskii, "Effect of high magnetic fields on phase transitions," *Fiz. Met. Metalloved.*, vol. 18, no. 4, pp. 502–505, 1964.
[17] D. M. C. Nicholson, R. A. Kisner, G. M. Ludtka et al., "The effect of high magnetic field on phase stability in Fe-Ni," *Journal of Applied Physics*, vol. 95, no. 11, pp. 6580–6582, 2004.
[18] K. Shimizu and T. Kakeshita, "Effect of magnetic fields on martensitic transformations in ferrous alloys and steels," *ISIJ International*, vol. 29, no. 2, pp. 97–116, 1989.
[19] H. Ohtsuka, "Structural control of Fe-based alloys through diffusional solid/solid phase transformations in a high magnetic field," *Science and Technology of Advanced Materials*, vol. 9, no. 1, Article ID 013004, 2008.
[20] H. D. Joo, S. U. Kim, N. S. Shin, and Y. M. Koo, "An effect of high magnetic field on phase transformation in Fe–C system," *Materials Letters*, vol. 43, no. 5-6, pp. 225–229, 2000.
[21] A. Ispas and A. Bund, *Proceedings of the Joint 15th Riga and 6th PAMIR International Conference on Fundamental and Applied MHD*, 2005.
[22] D. A. Allwood, G. Xiong, C. C. Faulkner, D. Atkinson, D. Petit, and R. P. Cowburn, "Magnetic domain-wall logic," *Science*, vol. 309, no. 5741, pp. 1688–1692, 2005.
[23] S. S. P. Parkin, M. Hayashi, and L. Thomas, "Magnetic domain-wall racetrack memory," *Science*, vol. 320, no. 5873, pp. 190–194, 2008.
[24] I. V. Vernyhora, D. Ledue, R. Patte, and H. Zapolsky, "Monte Carlo investigation of the correlation between magnetic and chemical ordering in NiFe alloys," *Journal of Magnetism and Magnetic Materials*, vol. 322, no. 17, pp. 2465–2470, 2010.
[25] V. A. Tatarenko and T. M. Radchenko, "The application of radiation diffuse scattering to the calculation of phase diagrams of F.C.C. substitutional alloys," *Intermetallics*, vol. 11, no. 11-12, pp. 1319–1326, 2003.
[26] S. M. Bokoch and V. A. Tatarenko, "A semi-empirical parameterization of interatomic interactions based on the statistical-thermodynamic analysis of the data on radiation diffraction and phase equilibria in f.c.c.-Ni–Fe alloys," *Solid State Phenomena*, vol. 138, pp. 303–318, 2008.
[27] S. M. Bokoch and V. A. Tatarenko, "Interatomic interactions in f.c.c.-Ni–Fe alloys," *Uspehi Fiziki Metallov*, vol. 11, no. 4, pp. 413–460, 2010.
[28] V. A. Tatarenko, S. M. Bokoch, V. M. Nadutov, T. M. Radchenko, and Y. B. Park, "Semi-empirical parameterization of interatomic interactions and kinetics of the atomic ordering in Ni–Fe–C permalloys and elinvars," *Defect and Diffusion Forum*, vol. 280-281, pp. 29–78, 2008.
[29] I. V. Vernyhora, S. M. Bokoch, and V. A. Tatarenko, "Interplay of magnetic and structural properties of f.c.c.-Ni–Fe alloys: study of statistical thermodynamics and kinetics by means of methods of computer simulation," *Uspehi Fiziki Metallov*, vol. 11, no. 3, pp. 313–368, 2010.
[30] A. G. Khachaturyan, *Theory of Structural Transformations in Solids*, Dover Publications, Mineola, NY, USA, 2008.
[31] A. A. Smirnov, *Molecular-Kinetic Theory of Metals*, Nauka, Moscow, Russia, 1966.
[32] A. G. Khachaturyan, "Ordering in substitutional and interstitial solid solutions," *Progress in Materials Science*, vol. 22, no. 1-2, pp. 1–150, 1978.
[33] J. S. Smart, *Effective Field in Theories of Magnetism*, W. B. Saunders Company, Philadelphia, PA, USA, 1966.
[34] A. Aharoni, *Introduction to the Theory of Ferromagnetism*, Oxford University Press, New York, NY, USA, 2000.
[35] Y. T. Millev and M. Fähnle, "No longer transcendentalequations in the homogeneous mean-field theory of ferromagnets," *Physica Status Solidi*, vol. 171, no. 2, pp. 499–504, 1992.
[36] Y. T. Millev and M. Fähnle, "On the mean-field treatment of ferromagnetic models with arbitrary anisotropy," *Physica Status Solidi*, vol. 176, no. 2, pp. K67–K69, 1993.
[37] Y. T. Millev and M. Fähnle, "A parametric solution to the general mean-field equation of ferromagnetism," *Physica Status Solidi*, vol. 182, no. 1, pp. K35–K38, 1994.
[38] Y. T. Millev and M. Fähnle, "A contribution to the mean-field analysis of amorphous magnets," *Physica Status Solidi*, vol. 179, no. 2, pp. 551–556, 1993.
[39] K. Ried, Y. Millev, M. Fähnle, and H. Kronmüller, "Renormalized field theory of the critical behaviour of anisotropic dipolar ferromagnets," *Physics Letters A*, vol. 180, no. 4-5, pp. 370–374, 1993.
[40] Y. T. Millev, H. P. Oepen, and J. Kirschner, "Influence of external field on spin reorientation transitions in uniaxial ferromagnets. I. General analysis for bulk and thin-film systems," *Physical Review B*, vol. 57, no. 10, pp. 5837–5859, 1998.
[41] http://www.magnet.fsu.edu/.
[42] T. Garcin, S. Rivoirard, and E. Beaugnon, "In situ characterizationof phase transformations in a magnetic field in Fe-Ni alloys," *Journal of Physics*, vol. 156, no. 1, Article ID 012010, 2009.
[43] T. Garcin, S. Rivoirard, and E. Beaugnon, "Thermodynamic analysis using experimental magnetization data of the austenite/ferrite phase transformation in Fe-xNi alloys ($x = 0, 2, 4$ wt%) in a strong magnetic field," *Journal of Physics D*, vol. 44, no. 1, Article ID 015001, 2011.
[44] Y. Ma, S. Awaji, K. Watanabe, M. Matsumoto, and N. Kobayashi, "X-ray diffraction study of the structural phase transition of Ni_2MnGa alloys in high magnetic fields," *Solid State Communications*, vol. 113, no. 12, pp. 671–676, 2000.